2013

Displacement profile estimation using low cost inertial motion sensors with applications to sporting and rehabilitation exercises

James Coyte
University of Wollongong, jlc978@uowmail.edu.au

David A. Stirling
University of Wollongong, stirling@uow.edu.au

Montserrat Ros
University of Wollongong, montse@uow.edu.au

Haiping Du
University of Wollongong, hdu@uow.edu.au

Andrew Gray
St George Illawarra Dragons Rugby Team

Displacement profile estimation using low cost inertial motion sensors with applications to sporting and rehabilitation exercises

Abstract

This paper investigates two methods of displacement estimation using sampled acceleration and orientation data from a 6 degrees of freedom (DOF) Inertial Measurement Unit (IMU), with the application to sporting training and rehabilitation. Currently, the use of low cost IMUs for this particular application is very impractical due to the accumulation of errors from various sources. Previous studies and projects that have applied IMUs to similar applications have used a lower number of DOF, or have used higher accuracy navigational grade IMUs. Solutions to the acceleration noise accumulation and gyroscope angle error problem are proposed in this paper. A zero velocity update algorithm (ZUPT) is also developed to improve the accuracy of displacement estimation with a low grade IMU. The experimental results from this study demonstrate the feasibility of using an IMU with loose tolerances to determine the displacement. Peak distances of a range of exercises are shown to be measured with accuracies within 5% for the numerical integration methods.

Keywords

estimation, profile, displacement, sporting, applications, sensors, motion, inertial, exercises, cost, rehabilitation, low

Disciplines

Engineering | Science and Technology Studies

Displacement Profile Estimation using Low Cost Inertial Motion Sensors with Applications to Sporting and Rehabilitation Exercises

James L.Coyte[1], David Stirling[1], Montserrat Ros[1], Haiping Du[1], Andrew Gray[2]

Abstract— **This paper investigates two methods of displacement estimation using sampled acceleration and orientation data from a 6 degrees of freedom (DOF) Inertial Measurement Unit (IMU), with the application to sporting training and rehabilitation. Currently, the use of low cost IMUs for this particular application is very impractical due to the accumulation of errors from various sources. Previous studies and projects that have applied IMUs to similar applications have used a lower number of DOF, or have used higher accuracy navigational grade IMUs. Solutions to the acceleration noise accumulation and gyroscope angle error problem are proposed in this paper. A zero velocity update algorithm (ZUPT) is also developed to improve the accuracy of displacement estimation with a low grade IMU. The experimental results from this study demonstrate the feasibility of using an IMU with loose tolerances to determine the displacement. Peak distances of a range of exercises are shown to be measured with accuracies within 5% for the numerical integration methods.**

I. INTRODUCTION

There is a high demand amongst performance athletes and rehabilitation trainers to track the displacement and velocity motion profiles of power lifting exercises in three dimensions. This allows for the trainer to perform a further quantitative analysis in order to prevent injuries and to maximise the efficiency of the exercises performed.

As IMU sensors are unable to measure position directly (only angular velocity and acceleration measurements), accurately determining the position of a rigid body using IMUs has been proven to be a challenge, especially in applications where the displacement is to be estimated over a long period of time, due to errors in the acceleration measurement accumulating [1]. However, IMUs have the advantages of low cost and high portability compared to optical sensors, which show that the IMU is a highly desirable option for this application [2].

Using direct numerical double integration, the error in the displacement will accumulate towards exponentially due to imperfections in the IMU (from accelerometer bias and gyroscope misalignments). In a study by Faulkner [3], the displacement of a repetitive motion is investigated and it is shown that the error in displacement calculation using direct integration with industrial grade quality sensors will exceed 1 metre after a period of 5 seconds has passed. Equation (1) is an approximation of the accelerometer error accumulation

where δx is displacement error and $\delta \ddot{x}$ is acceleration error. A solution presented to solve this problem was the use of a real-time zero velocity update algorithm (ZUPT) which detects the point in time when the incremental velocity should be zero by using an algorithm that detects the anticipated end point of the repetitive motion and binds the acceleration profile to zero. This method is practical under the condition that the initial and final velocities are equal to zero and that the acceleration profile for each repetition is of similar shape geometrically.

Examples of commonly used ZUPT algorithms for detecting the stationary points of repetitive motions using an IMU include the use of hidden Markov models [4], to identify the periods. Other methods use statistical variance and norm of a particular component of the motion to calculate the zero velocity thresholds [5].

$$\delta x \cong \frac{1}{2} \delta \ddot{x} t^2 \tag{1}$$

A method of removing the accelerometer drift error from the data is the use of least squares method to remove the linear trend from the data series. The main disadvantage of this method is that outlying data points in the acceleration profile can interfere with the trend line and give an inaccurate result [6] [7].

An alternative displacement estimation method involves the use of Fourier analysis to decompose the acceleration waveform into an equivalent series of sinusoidal waveforms. If the parameters of a sinusoidal function are known, then the exact value of the double integral can be calculated with the use of a trigonometric anti-derivative identity.

Equation (2) shows this relationship in the frequency domain. This particular method is accurate for analysing particles in simple harmonic motion, since the motion profile of the particle can be represented by a single sinusoidal function. However, if there is a zero or low frequency component, then it will need to be processed separately. Once the Fast Fourier Transform (FFT) of the sampled data is performed, each term can then be divided by its own frequency squared, then finally transformed back into the time domain to provide a displacement profile as a function of time. A drawback with this method is that the sampling rate of the reconstructed signal will be half of the sampling rate of the sampled data (caused by the inclusion of negative frequencies); this can result in aliasing of the reconstructed time signal after performing the inverse Fast Fourier transform (IFFT). The frequencies will need to be scaled to produce an accurate result [8].

1 School of Electrical, Computer and Telecommunications Engineering Wollongong, 2500 Australia (first author's e-mail: jlc978@uowmail.edu.au).
2 St George Illawarra Dragons, Wollongong NSW 2500

$$X(j\omega) = \frac{\ddot{X}(j\omega)}{-\omega^2} \qquad (2)$$

Programming the standard discrete Fourier transform on a computer using the FFT formula directly will require the calculation of N^2 complex algebra operation which will consequently require a larger number of resources and more time to calculate (N is the length of the data series). The Cooley Tukey algorithm is a more efficient method requiring $2N \log_2 N$ number of operations [9].

Data mining and machine learning have a wide variety of applications. When processing signal data problems may be encountered that are difficult to solve on a computer using the Newtonian equations of motion directly, for example the filtering of high frequency vibrations and compensating for rotating accelerometer biases.

There is an alternative version of the successful C4.5 algorithm for the top down induction of decision trees that has been ported into Java as J48 [10]. The Weka application provides a platform with several machine learning algorithms including J48. Using labeled sensor training data it can define a set of rules that will make decisions based on patterns that occur in the data [11]. The intended contribution of this paper is to use machine learning to develop a new algorithm for detecting in each phase of the weight lift. This will aid in compensating for accelerometer and gyroscope errors for low cost IMUs.

This paper is organized as follow: Section II of this paper addresses the design problem that is solved by the concepts in this research project. Section III gives details on the theoretical concepts that are applied in this project. Section IV outlines the experimental procedure and presents the results. The conclusions are given in section V.

II. PROBLEM DEFINITION

The main objective of this study was to investigate the feasibility of a flexible 6 DOF inertial motion tracking system for weight training exercises with a barbell i.e. the vertical component of motion can be detected and analysed separately regardless of the orientation of the barbell at any point of time during the exercise.

The general objective is to use a low grade IMU that is burdened by a large margin of error, in order to reduce costs, to accurately measure displacements with the use of a software application to process the data and to calibrate the device. Given in the study by Faulkner [3] showed the displacement error caused by the double integration of the acceleration bias has a time squared relationship.

The two weight lift exercises analysed in this work are the "dead lift" and the "squat". Both exercises are performed using a typical training gymnasium barbell.

The deadlift exercise (shown in Fig.1) involves the athlete lifting a barbell loaded with weights from the ground starting in a bent-over position and lifting the weight vertically. The dead lift motion itself is considered to be purely "concentric" (the phase where the muscles are purely in contraction). The beginning of this lift phase is considered to be the most physically demanding [12].

The squat weight exercise is a weight lift that mainly trains the thigh and quadriceps as well as many more muscles such as abdominals, shoulders and back muscles. This exercise is performed by holding the bar at the back of the neck. The weight lifting motion of the squat begins from the standing position then the hips are lowered with the torso as shown in Fig.2. Then afterwards, the athlete returns back to the upright position [13].
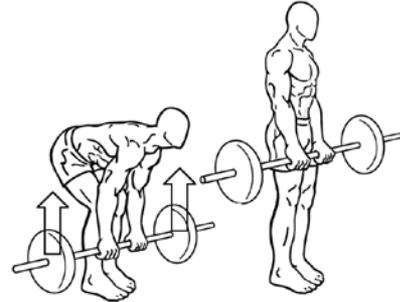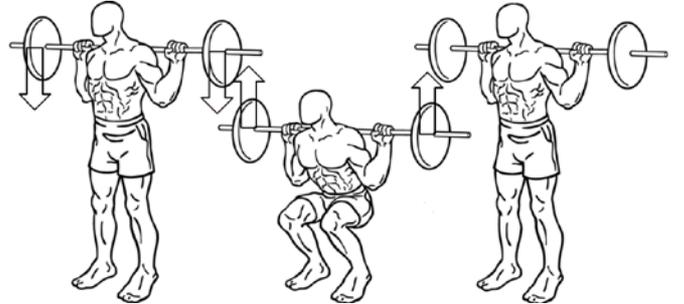

Fig. 1 The dead lift motion [14].

Fig. 2 The squat motion [14].

III. NEW ALGORITHM DESIGN

The software design for this motion tracking system requires techniques including analytical mechanics, data mining and signal processing. A machine learning technique is used to develop a decision based algorithm to activate the calibration procedure and set the velocity to zero when the ZUPT period occurs. The displacement profiles are then estimated using two different methods: numerical integration and frequency integration.

A. Obtaining the vertical component of motion

The barbell used in the gymnasium environment will be assumed to be unconstrained from the ground frame. All frames and barbell material itself will be analysed as a rigid body. The sensor coordinate frame will then be free to rotate in any direction relative to the ground frame. The ground frame is assumed to have the z axis constrained to the same direction as the vector of the acceleration due to gravity. The x and y axes are positioned perpendicular to the gravity vector.

In order to measure the acceleration in the true vertical direction, a rotation matrix (that will transform the initial sensor frame coordinates to the frame relative to ground)
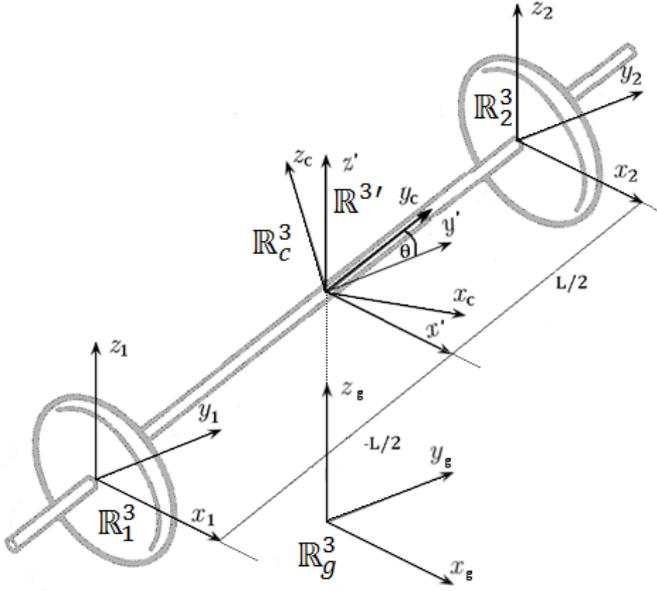
Fig. 3. The definition of the coordinate systems

must be calculated during the calibration step. The initial acceleration vector measured from the central coordinate system $\mathbb{R}^3_c$ is given in Eq. (3) as vector $\hat{a}_{C0}$ whose values are initially unknown. During the static calibration phase, the magnitude of this vector will equal the vertical component $\ddot{z}'_{g0}$ of the $\mathbb{R}^3_g$ system, which is equal to acceleration due to gravity shown in Eq. (4). Since the values of the vectors $\hat{a}'_0$ and $\hat{a}_{C0}$ are now known, the matrix R_{cal} then can be determined by solving Eq. (6). R_{cal} is a 3-by-3 rotation matrix.

$$\hat{a}_{C0} = \{\ddot{x}_{C0}, \ddot{y}_{C0}, \ddot{z}_{C0}\} \tag{3}$$

$$|\hat{a}'_0| = \ddot{z}'_{g0} = \{0, 0, |\hat{a}_{C0}|\} \tag{4}$$

$$|\hat{a}'_0| \cong 9.81 m/s^2 \tag{5}$$

$$\hat{a}'_0 = R_{cal} \times \hat{a}_{C0} \tag{6}$$

During the measurement phase, the acceleration vector measured from the sensor frame is then sequentially rotated by R_{cal} and transformed by the inverse orientation of the coordinate system $\mathbb{R}^3_c$. This is necessary, in order to measure the acceleration relative to the ground frame whilst the sensor frame is rotating.

The individual motion profile of the mass at each end can be calculated geometrically using the difference in the orientation ($R_c(\theta, \phi, \psi)$) between the ground frame and the sensor frame (as shown symbolically in Eq. (7)).

$$\begin{bmatrix} x_{1,2} \\ y_{1,2} \\ z_{1,2} \end{bmatrix} = R_c(\theta, \phi, \psi) \times \begin{bmatrix} x_c \\ y_c \pm \dfrac{L}{2} \\ z_c \end{bmatrix} \tag{7}$$

B. Zero Velocity Update Classification Using Machine Learning

A zero velocity update is used to identify when the sensor is stationary. The initial and final values of the acceleration and velocity waveform are then subsequently set to zero. The zero velocity update classifier was designed using a machine learning induction algorithm (J48 which is an open source version of the C4.5 algorithm). The sampled acceleration and the calculated jerk data was input as the training data and a Boolean series was input as the class. The Boolean data defined when the corresponding acceleration and jerk data was representing the lifting and lowering motion.

The resultant decision trees, illustrated in Fig.4 will assert that the barbell is stationary when the outputs of both the jerk and acceleration decision trees are equal to "zero velocity". The "jerk" also known as the derivative of acceleration, is denoted by $\dddot{z}'$. In the stationary condition, the velocity and the acceleration measurements can be reset to zero. The coordinate system calibration procedure (outlined in section III.A.) is performed during every zero velocity update interval in order to minimise the angle error caused by the axes misalignment. This is necessary because the grade of IMU selected for this application is also afflicted by gyroscope errors of up to 5 degrees.
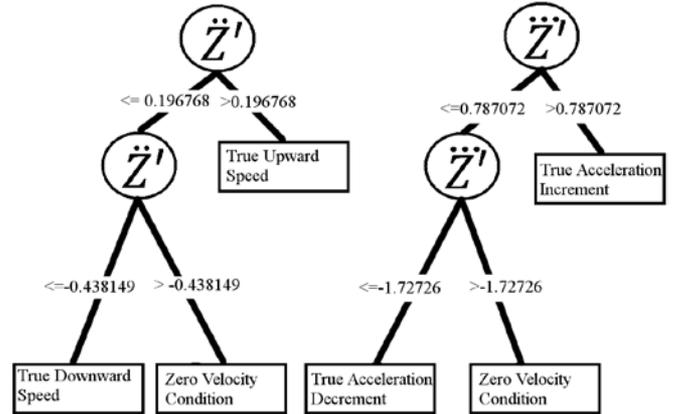

Fig. 4. Decision trees for the dead lift zero velocity update data classifier

An alternative method for removing the acceleration accumulative error is the use of a least squares filter to remove the linear trend from the data series. A comparison in the results of these two methods is given in Fig.5. It can be observed that the de-trend method skews the peaks of the velocity waveform where as the decision based tree preserves the data and sets the initial and final values exactly to zero. This will be discussed further in section IV.B.

C. Displacement Estimation Method 1: FFT/IFFT Frequency Integration Method

By inspection, the weight lifting acceleration wave form resembles a non ideal particle vibrating in simple harmonic motion. The main purpose of using this method is to avoid the accelerometer drift error. The FFT method used in this study is the Cooley Tukey algorithm [9].
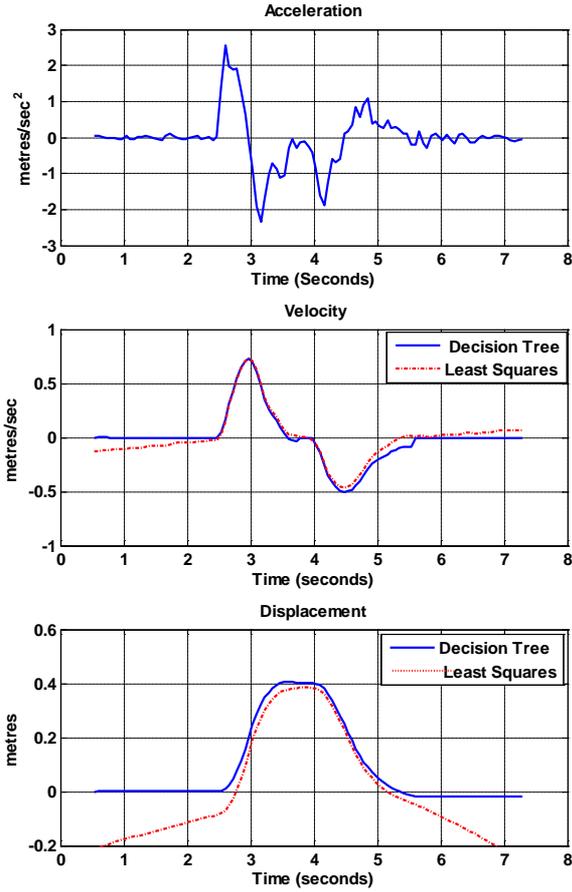
Fig. 5. The acceleration, velocity and displacement profiles for a single dead lift, using numerical integration with zero velocity update and least squares filtering.

The relationship between the oscillatory displacement $x(n)$ and the sequence of acceleration data in the frequency domain is given in Eq.8 which is based on the double anti derivative rule for trigonometric functions. The acceleration data is transformed to the frequency domain $\ddot{X}(k)$ and is then each kth term is then divided by negative kth frequency squared. The β term is a frequency scaling factor which is used to compensate for the accelerometer error. This equation will only produce a valid result if the zero frequency component is a value close to zero. Equation (9) is the nth root of unity which is substituted in Eq. (8) to transform the signal to the discrete time domain.

$$x(n) = \frac{1}{N} \sum_{k=1}^{N} \frac{\ddot{X}(k)\omega_N^{-(n-1)(k-1)}}{-(2\pi k\beta\Delta f)^2} \qquad (8)$$

$$\omega_N = e^{\frac{-2\pi j}{N}} \qquad (9)$$

D. Displacement Estimation Method 2: Direct Integration

The discrete integration formula used in this application is given in Eq.(10) and Eq. (11) are based on the trapezoid rule, where T_s is the sampling period. Equation (10) gives

the discrete velocity. The initial values $x(0)$ and $\dot{x}(0)n$ are zero under ideal conditions.

$$\dot{x}(n) = x(0) + \sum_{n:1\to\infty}^{\infty} \frac{\ddot{x}(n-1) + \ddot{x}(n)}{2} T_s \qquad (10)$$

$$x(n) = \dot{x}(0)n + \sum_{n:1\to\infty}^{\infty} \frac{\dot{x}(n-1) + \dot{x}(n)}{2} T_s \qquad (11)$$

IV. EXPERIMENT

A. Methodology

The experiment was performed using a replica barbell. The material of the bar used was a Steel Alloy SAE1018 (composition includes: 0.18% Carbon, 99% Ferrite). The dimensions used are 12mm Diameter, and Length L = 1.5m. The sensor was fastened to the centre of the bar and two 3Kg weights were affixed to each end of the bar.

Table 1 Summary of the Key Technical Specifications for theUM6 Ultra Mini IMU by CHRobotics.

Parameter	Value
Max Sample rate	500Hz Gyros
	300Hz Accelerometers
Acceleration Dynamic Range	$\pm19.6 m/s^2$
Angular velocity Dynamic Range	$\pm2000\,°/s$
pitch and roll angle accuracy	$<2°$
yaw angle accuracy	$<5°$

The brand of the sensor used was the UM6 Ultra Mini IMU sensor. Device specifications are given in Table 1. Before sampling data from the device a calibration procedure was performed to compensate for the magnetic field distortions caused by the iron in the steel barbell, using the extended Kalman filter. Calibration procedures were also applied to compensate for interference caused by temperature (these calibration procedures are given in the manufacturer's data sheet) [15].

The accelerometer, quaternion position estimates and the gyroscope velocity data was logged from the device via serial communication during the test procedure of 10 repetitions of each exercise. The peak distance of the squats and dead lifts were also measured with a metre ruler to create a reference point that the results can be compared against to calculate the error.

B. Dead lift Results Summary

A sample of the results for the dead lift exercise is given in Fig. 5. The plot illustrates the relationship between the acceleration, velocity and displacement for a single
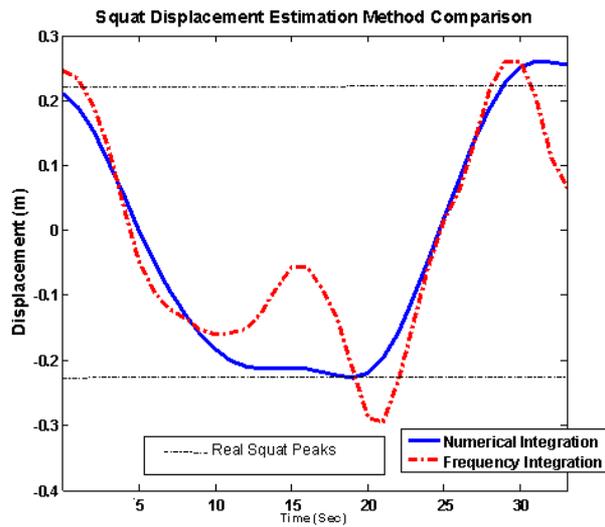
Fig. 6 Comparison between displacement estimation methods and a measured reference point of 0.45m.
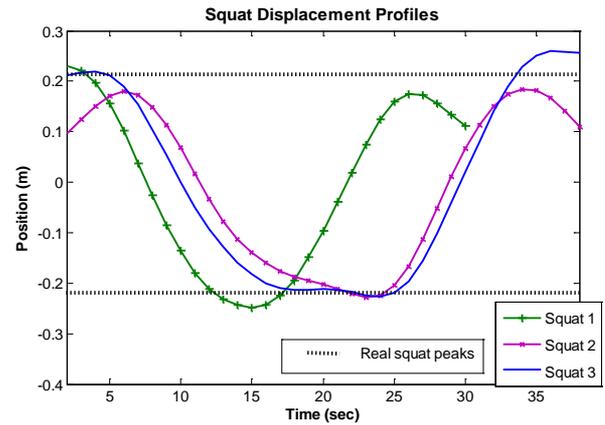

Fig. 7. Three squat displacement profiles compared to a measured reference point of 0.45m using the numerical integration method.

Table 2 peak error for each method of filtering and integration

Filter	Decision Tree Filtering (ZUPT)				Least Squares Filtering			
	Average Absolute error $(10^{-3}m)$		Average Relative error (percent)		Average Absolute error $(10^{-3}m)$		Average Relative error (percent)	
Integration Method	Numerical Integration	Frequency Integration	Numerical Integration	Frequency Integration	Numerical Integration	Frequency Integration	Numerical Integration	Frequency Integration
Dead lift	31.8	n/a	5.29%	n/a	64.9	n/a	9.54%	n/a
Squat	10.6	31.9	4.71%	14.18%	38.39	44.83	17.77%	19.92%

repetition. It can be noted that the displacement curve does not return precisely to zero due to the error in accelerometer integration. It can also be noted that the later part of the profile after 5 seconds is plagued with small vibrations that slowly taper down. This is due to the barbell making impact with the ground and vibrating at a high frequency. It is speculated that these vibrations are under sampled, which can result in a greater error in the velocity and displacement estimation. The dead lifts produced poor results with the frequency integration method, with an error greater than 100%. The result of the least squares filter is compared to the decision tree zero velocity update algorithm that is designed in section III.B.

C. Squat Results Summary

Unlike the dead lift, the entire motion of the squat is undertaken in the grasp of the weight lifter so there are no major impact forces that cause high frequency vibrations.

The analysis of the waveforms produced with the squat exercise yielded similar results for both the frequency domain integration method and the numerical integration method. Fig.6 shows the graphical comparison between the two displacement estimation methods. By visual observation, the peak to peak results obtained from the numerical integration method are much closer to the measured reference value. The waveform of the frequency domain method is shown to overshoot the reference value due to the Gibbs Phenomenon. Fig.7 shows a plot of three squat repetitions to illustrate the difference between the measured reference point ("real squat peaks") and the maximum and minimum values of the displacement profile, this difference is the absolute error.

A. Error Comparison

The error from the results of the 20 repetitions of dead lifts and squats were calculated using the distance measured by a metre rule as a set point compared to the distance between maximum and minimum value that is estimated. The relative error and the absolute errors were calculated and are shown in Table 2. The accuracy of the filtering methods: Decision Tree Filtering (ZUPT) and the least squares method are compared, as well as the two displacement estimation methods. The numerical integration method produced similar levels of accuracy for each exercise. The frequency domain integration method error was omitted for the dead lift because it produced results with a very large error

(greater than 100%) due to the high frequency vibrations caused by the impact of the floor on the barbell.

V. CONCLUSION

The feasibility of using low grade IMUs to calculate the displacement waveforms for analysing the physical properties of human motion is verified.

With the use of the decision tree ZUPT, the numerical integration method gave similar results for both the dead lifts and squat exercises with accuracies of 5.29% and 4.71% respectively. There was a slightly higher accuracy in peak to peak displacement estimation when compared to the frequency domain integration method for squat exercises with an accuracy of 14.18%. The frequency integration method produced unreliable results for the dead lift exercise.

The least squares method of filtering gave results with a larger error in the estimated values when compared to the ZUPT decision tree filter. The numerical integration method produced results with an error of 9.54% and 17.77% for the dead lifts and squats calculated. The frequency integration method gave results with an error of 19.92% for the squats. It is noted that the least squares filter gave more accurate results for the dead lifts than the squats.

In the experiments undertaken in this study, the accuracy of the slope and inflexions of each displacement curve was not tested, only the magnitude of the displacement for each exercise was compared to a measured reference point. Further investigation could be performed using optical sensors to determine how accurate the other geometric properties of the displacement profiles are as estimated by the methods described in this paper.

There is further potential to perform work with the data classification techniques to identify the lowering, lifting and the impact force region of the acceleration motion profile separately, to help remove the under sampled vibrations from the dead lift data.

REFERENCES

[1] O. Wongwirat and C. Chaiyarat, "A Position Tracking Experiment of Mobile Robot with Inertial Measurement Unit (IMU)," *International Conference on Control, Automation and Systems,* pp. 27-30, October 2010.

[2] M. Field, Z. Pan, D. Stirling and F. Naghdy, "Human motion capture sensors and analysis in robotics," *Emerald Article: Human motion capture sensors and analysis in robotics,* pp. 163 - 171, 2011.

[3] W. T. Faulkner, R. Alwood and D. Bohlin, "Altitude Accuracy While Tracking Pedestrians Using a Boot-mounted IMU," in *Position Location and Navigation Symposium (PLANS)*, Springfield, VA, USA, 2010.

[4] S. K. Park and Y. S. Suh, "A zero velocity detection algorithm using inertial sensors for pedestrian navigation systems," *Sensors (Switzerland),* vol. 10, no. 10, pp. 9163-9178, 2010.

[5] E. Foxlin, "Pedestrian tracking with shoe-mounted inertial sensors," *IEEE Computer Graphics and Applications,* vol. 25, no. 6, pp. 38-46, 2005.

[6] J. Hwang, H. Yun, S.-K. Park and D. L. a. S. Hong, "Optimal Methods of RTK-GPS/Accelerometer Integration to Monitor the Displacement of Structures," *Sensors 2012,,* pp. 1014-1034, 2012.

[7] P. Esser, H. Dawes, J. Collett and K. Howells, "IMU: Inertial sensing of vertical CoM movement," *Journal of Biomechanics,* pp. 1578-1581, 2009.

[8] Colin Mercer, "Acceleration, Velocity and Displacement Spectra – Omega Arithmetic," *Prosig Signal Processing Tutorials,* 2006.

[9] J. W. Tukey and J. Cooley, "An Algorithm for the Machine Calculation of Complex Fourier Series," *Mathemarics of Computation,* no. 19, April 1965.

[10] J. Quinlan, "C4.5 Progress for Machine Learning," *Morgan Kaufmann Publishers Inc.,* 1993.

[11] M. Hall, E. Frank, G. Holmes, B. Pfahringer, P. Reutemann and I. H. Witten, "The WEKA Data Mining Software: An Update," *SIGKDD Explorations,* vol. 11, no. 1.

[12] musclestrong, "http://musclestrong.com/2010/11/21/deadlifts/," 11 2010. [Online].

[13] M. Rippetoe, Starting Strength: Basic Barbell Training, The Aasgaard Company, 2007.

[14] Everkinetic, "Weight lifting clip art Wikimedia Commons http://commons.wikimedia.org Image licensed under the Creative Commons Attribution-Share Alike 3.0 Unported (The sharing and producing adaptations of these images is permitted)," 2010.

[15] C. Chamberlain, 4 2012. [Online]. Available: www.chrobotics.com/.